

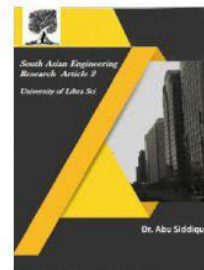


2581-4575

International Journal For Recent Developments in Science & Technology



A Peer Reviewed Research Journal



MONITORING OF SUBSIDENCE ALONG JINGJIN INTER-CITY RAILWAY WITH HIGH-RESOLUTION

M.VISHNU TEJA, D.CHANDRASEKAR, SK.SAMEER PASHA

Department of Mining Engineering, Malla Reddy Engineering College (Autonomous)

ABSTRACT

Improvement of railway capability results in heavier axle loads and higher speed lines, which further induces railway subsidence. In order to ensure a good railway performance and reduce railway life cycle costs, railway subsidence should be measured regularly. The paper aims to assess railway performance by monitoring land subsidence along the railway, predicting railway subsidence in the future based on historical subsidence records. Persistent Scatterer Interferometric Synthetic Aperture Radar (PS-InSAR) is adopted in this research for monitoring land subsidence along the railway while Autoregression Moving Average (ARMA), artificial neural network and grey model are applied for subsidence prediction. However, for the successful interpretation of the observed deformation within a structure, or between structures, it is imperative to associate a radar scatterer unambiguously with an actual physical object. Unfortunately, the limited positioning accuracy of the radar scatterers hampers this attribution, which limits the applicability of MT-InSAR.

INTRODUCTION

Railway systems consist of a complex collection of constructions, such as embankments, tunnels and bridges, subject to changing environmental conditions (geology, relief). As a result, several processes impact the structural health of these networks, depending on their locations. Examples are the differential subsidence of assets in soft soils, slope instabilities/slow landslides in mountainous areas, embankment instabilities, and aging and degradation of concrete constructions. Due to the foundation and construction of a railway section, several processes may occur on a very local scale. For example, in soft soils, the embankment with the rails may show a different deformation behavior compared to the catenary poles. Significant differential settlements have been observed in the transition zones relative to

fixed structures. Current approaches for structural health monitoring are

levelling, linear variable differential transformers and video based systems. While the latter can be used to monitor dynamic displacements, their applicability is limited due to manual operation and localized implementation. MT-InSAR is complementary to these in situ techniques and has the advantage of wide area applications, frequent revisits, and a millimeter level precision.

For a proper analysis and interpretation of MT-InSAR products, the locations of the coherent scatterers (CS) need to be known with at least decimeter level precision. Unfortunately, whereas the relative displacements with MT-InSAR is estimated with millimeter-level precisions, the positioning precision of radar scatterers is

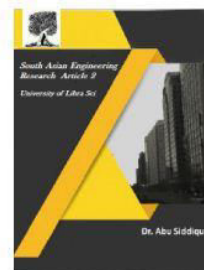


2581-4575

International Journal For Recent Developments in Science & Technology



A Peer Reviewed Research Journal



usually poor, in the order of meters. As a consequence, it is difficult to link the radar scatterers to the ground objects, which hampers the interpretation of the deformation signal and limits the applicability of MT-InSAR. The positioning accuracy of CS is dependent on: (i) factors influencing all CS systematically; and (ii) factors specific for each individual CS. The largest systematic uncertainty is introduced by the unknown absolute height of the reference CS. If a corner reflector or radar transponder is available for the whole time series, the reference height offset can be estimated by measuring its position. However, often such a device is not available. Airborne LiDAR provides 3D point clouds with very high spatial density, thus LiDAR points can be found close to all radar scatterers, which makes it attractive to estimate the systematic MT-InSAR height offset based on the full CS dataset.

Poor spatial resolution has been one of the main drawbacks of SAR data until recently. The launch of a new generation of high-resolution SAR satellites has dramatically increased the level of detail visible in SAR images. A high density of PS points can be detected, and more precise subsidence monitoring information extracted with high-resolution SAR data. Utilizing a high-resolution of 1 m and a short revisit time of 11 days offers a chance for TerraSAR-X (TSX) data to identify targets that need detailed information. The subsidence along subway tunnels and several highways in Shanghai was monitored with time series InSAR data collected by COSMO-SkyMed satellites. The high-resolution data of 3 m reveals impressive details of the ground surface deformation. TomoSAR with higher-order permanent scatterers analysis was found to be a useful way to interpret the height and

deformation of building areas, especially for very high buildings. Meanwhile, X-band PSI analysis makes possible the analysis and interpretation of the thermal expansion signal of single objects like buildings and bridges. Moreover, an extended PSI model was presented and a new PSI product, the thermal expansion map, was generated. Building facades were proven to be reconstructed by multiview TomoSAR point's clouds.

Notwithstanding the great efforts made in seeking the best approach, MT-InSAR technology is still far from being adopted as an operational tool for the monitoring of subsidence along a railway. One practical issue is that there is little chance to assess the high-density leveling campaign along LMLFs to validate the time series results of MT-InSAR analysis. In this paper, the research carried out on MT-InSAR analysis along Jingjin Inter-City railway is introduced. First, the potential of TSX data for the monitoring of subsidence along a high-speed railway is explored. Second, an estimate of the precision of the monitoring of subsidence with high-resolution MT-InSAR is analyzed and validation of the leveling data of high spatial/temporal sampling along Jingjin Inter-City railway is made. TSX MT-InSAR analysis was carried out by using SARPROZ. The output of the work will be useful to provide reference and will be helpful for further planning of subsidence monitoring over LMLFs.

The methods used to predict land subsidence can be divided into three main types: classical layer-wise summation, numerical calculation based on consolidation theory, and curve fitting. Curve fitting, which makes use of a mathematical formula to acquire a curve that best fits the field data and

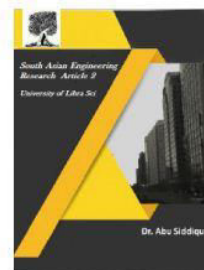


2581-4575

International Journal For Recent Developments in Science & Technology



A Peer Reviewed Research Journal



precisely reflects real world land subsidence, is used in many projects. In this paper, we analyze the performance of four frequently used curve fitting methods (Zhou et al. 2010; Wang 2009): hyperbola, expanded hyperbola, three-point fitting and the Asaoka method. The research of Chen Shanxiong suggests that expanded hyperbola matching possesses a higher correlation coefficient yet larger relative error than hyperbola fitting, while the Asaoka method may not apply in certain soil conditions despite strong correlation coefficients.

A number of methods for predicting land subsidence and monitoring deformation under high speed railway tracks exist, and are divided into three categories: layer-wise summation, numerical calculations based on consolidation theory, and curve fitting. One of these, curve fitting, including the hyperbola, expanded hyperbola, three-point fitting and Asaoka methods, is widely used because it is computationally simple and applicable in many situations. In this paper, we analyze the performance of the four classical curve fitting methods using field data and propose a novel approach to estimate land subsidence. The new method integrates three-point fitting, which is computationally simple whilst stringent in terms of correlation restrictions, with the Asaoka method to significantly improve performance in practical applications.

Railway Subsidence Prediction:

Railway subsidence monitoring over a certain period can be considered as typical discrete time series. Therefore, most of standard time series prediction approaches can be utilized to forecast its future subsidence. In general, these methods can be divided into statistical models and non-statistical models. Auto-regressive moving average (ARMA) can

be categories as the former, while neural network (NN) models based on artificial intelligence are representative of the latter. Furthermore, in early 1980's, a new predictive analysis methodology called grey system theory was introduced by Deng. It is capable of handling time series that have limited number of observations and contain unknown parameters and inter-relationships.

The profile function and influence function methods are now widely employed in all methods due to their practicality and ease of use. For conditions in which the topsoil is thick and the overburden strata include no ultra-thick and hard stratum (UTHS), the aforementioned methods have relatively high precision for predicting surface subsidence. However, for overburden strata with UTHS, the prediction results often differ greatly from measured results. For example, when mining under the ultra-thick igneous rock of the Haizi Coal Mine, the predicted maximum surface subsidence value obtained using influence function methods was significantly larger than the measured value (1270 mm versus 457 mm, respectively). This occurs because most of the above prediction methods consider the overburden strata as a homogenous medium. When the composition of the overburden strata is fairly uniform, this simplification is reasonable. However, surface subsidence is the result of a gradual development of overburden strata from bottom to top after mining, and different compositions of overburden strata have strong impacts on surface subsidence. Although the existing prediction methods take into account the influence of lithology of overburden strata on surface subsidence when choosing the prediction parameters, consideration of overburden remains insufficient.

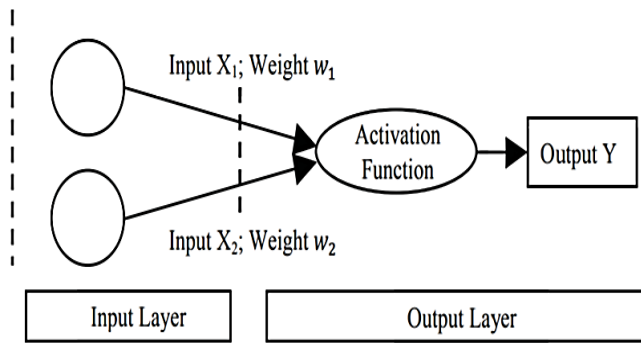
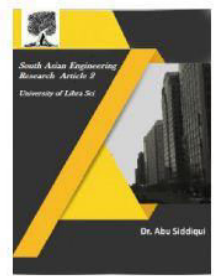


2581-4575

International Journal For Recent Developments in Science & Technology



A Peer Reviewed Research Journal



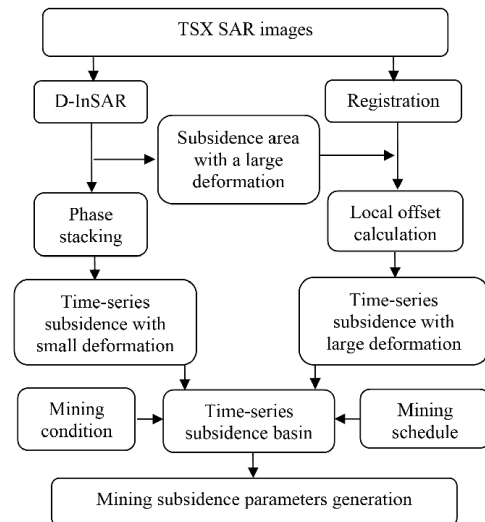
Layer artificial neural network

Subsidence is a global problem and, in the United States, more than 17,000 square miles in 45 States, an area roughly the size of New Hampshire and Vermont combined, have been directly affected by subsidence. More than 80 percent of the identified subsidence in the Nation has occurred because of exploitation of underground water, and the increasing development of land and water resources threatens to exacerbate existing land-subsidence problems and initiate new ones. In many areas of the arid Southwest, and in more humid areas underlain by soluble rocks such as limestone, gypsum, or salt, land subsidence is an often-overlooked environmental consequence of our land- and water-use practices.

When you look at the photo below of the Basilica in Mexico City, do you find yourself asking if it might not look straight? In fact, the foundation of the Basilica on the left is sinking and this sinking phenomenon is happening throughout Mexico City, where long-term extraction of groundwater has caused significant land subsidence and associated aquifer-system compaction, which has damaged colonial-era buildings, buckled highways, and disrupted water supply and waste-water drainage. Some buildings have been deemed unsafe and have been closed and

many others have needed repair to keep them intact.

FLOWCHART



METHODOLOGY

After PS detection, all PSs are connected to form a Delaunay triangulation network, which is taken as the subsidence observation network. Phase modeling is based on the concept of neighborhood differencing applied to each of the links in the Delaunay triangulation network.

Given N differential interferograms, the phase values at two neighboring PSs (e.g., p and q) extracted from the its differential interferogram can be expressed by

$$\Phi_i^p = -\frac{4\pi B_i^T}{\lambda} v_p \cos \theta_p - \frac{4\pi B_{i,p}^\perp}{\lambda R_p \sin \theta_p} \varepsilon_p + \hat{\phi}_i^p - 2k_p \pi,$$

$$\Phi_i^q = -\frac{4\pi B_i^T}{\lambda} v_q \cos \theta_q - \frac{4\pi B_{i,q}^\perp}{\lambda R_q \sin \theta_q} \varepsilon_q + \hat{\phi}_i^q - 2k_q \pi,$$

where Φ_i^* is the wrapped phase at the PSs; v^* and ε^* are the subsidence rates and the elevation residuals (due to uncertainties in the SRTM DEM used) at the PSs, respectively; B_i is the TB of the i th interferogram; $B_{i,*}^\perp$ is the SB of the PSs in the i th interferogram; λ is the radar wavelength (3.1 cm for the TSX

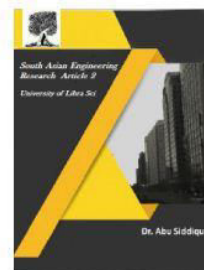


2581-4575

International Journal For Recent Developments in Science & Technology



A Peer Reviewed Research Journal



system); R^* and θ^* are the sensor-to-target range and the radar incident angle at the PSs, respectively; $\phi_{\text{res},i}$ is the residual phase consisting of the nonlinear subsidence, atmospheric artifacts, orbit errors, and decorrelation noises; and $2k\pi$ denotes the integer ambiguity of the wrapped observation phases.

After neighborhood differencing, the phase increment ($\Phi_{\text{diff},i}$) between the two adjacent PSs of each link can be derived by using Eqs. (2) and (3) and represented as a function of the subsidence rate increment (v), the elevation residual increment (ξ), and the residual phase increment ($\phi_{\text{res},p,q,i}$) [12]. N differential equations can be obtained by using N differential interferograms. In each link, v and ξ can be estimated by maximizing the following objective function.

$$\begin{cases} \gamma = \max \left[\left| \frac{1}{N} \sum_{i=1}^N (\cos \omega_i + j \sin \omega_i) \right| \right] \\ \omega_i = \tilde{\phi}_i - \frac{4\pi B_{\perp}^i}{\lambda} v \cos \bar{\theta} - \frac{4\pi \bar{B}_i}{\lambda R \sin \bar{\theta}} \xi, \end{cases}$$

where R^- , θ^- , and B_{\perp}^- are the mean sensor-to-target range, the mean radar incident angle, and the mean perpendicular baseline between two PSs, respectively; γ is the model coherence (MC) of the link; and $j = -1 \dots \sqrt{1}$. v and ξ can be derived by searching within a given solution space (e.g., -5 to 5 mm/year for v and -20 to 20 m for ξ when high-resolution TSX images are used) to maximize the MC. In this study, the searching procedure was carried out with step values of 0.01 mm/year and 0.02 m for v and ξ , respectively.

Once the subsidence rate and elevation residual increments of all the links are estimated, the Delaunay triangulation network can be treated by the weighted least squares (LS) adjustment to estimate the subsidence rates and the elevation residuals of all the PSs.

The square of the maximized MC value of each link is considered the weight. An LP with subsidence rate obtained through leveling measurements can be considered as a reference point for the LS adjustment. In this paper, we focus on analyzing the PSI-retrieved subsidence along road networks. A detailed discussion on PSI approach is beyond the scope of this work and can be found.

CONCLUSION

A time series analysis of railway subsidence is carried out based on the application of PS-InSAR which provides a method for land subsidence monitoring over large coverage and long time span. Railway sections with serious subsidence are selected for more frequent subsidence monitoring. Based on the historical subsidence information acquired from PSInSAR, railway subsidence can be predicted by ARMA, artificial neural network and grey model and a railway maintenance plan will be established according to the prediction result. Apart from railway subsidence monitoring and prediction, safety assessment of railway infrastructure should be considered as the future work for an integrated approach of railway performance assessment. Wet weather has already affected the infrastructure of both railway and highway in the UK. For instance, wet weather resulted in a 15 ft-deep sinkhole on M2 near Sittingbourne in 2014. In addition, land subsidence occurred at London Jubilee Tube Extension Line due to water extraction.

As a result, a safety assessment which considers factors that might threaten the stability of railway infrastructure should be adopted. The factors which have the most significant contribution on infrastructure deterioration will be identified through fuzzy logic model and neural network. Generally

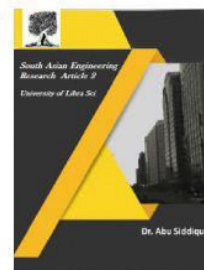


2581-4575

International Journal For Recent Developments in Science & Technology



A Peer Reviewed Research Journal



speaking, risk level of a safety factor is determined by its frequency of occurrence and consequence severity. However, frequency and severity of some factors related to railway infrastructure are uncertain, fuzzy logic model can be adopted to assess safety by identifying risk level and risk degree of the factors. Railway safety level can be also assessed based on a comprehensive evaluation on factors that have influential impact on railway safety together with their corresponding weights in the total contribution to railway safety. Artificial neural network model has been demonstrated to be capable of determining these weights through its various learning algorithms and processes.

REFERENCES

1. Yu, Q.; Wang, W.; Yi, C. Design and Application of an Automatic System for Land-subsidence and Water Table Monitoring in Tianjin City. *Ground Water* 2007, 29, 101–104.
2. Zhou, G.; Yan, H.; Chen, K.; Zhang, R. Spatial analysis for susceptibility of second-time karst sinkholes: A case study of Jili Village in Guangxi, China. *Comput. Geosci.* 2016, 89, 144–160. [CrossRef]
3. Liu, G.X.; Jia, H.G.; Zhang, R.; Zhang, H.X.; Jia, H.L.; Yu, B.; Sang, M.Z. Exploration of Subsidence Estimation by Persistent Scatterer InSAR on Time Series of High Resolution TerraSAR-X Images. *IEEE J. Sel. Top. Appl. Earth Obs. Remote Sens.* 2011, 4, 159–170. [CrossRef]
4. Luo, Q.; Perissin, D.; Li, Q.; Lin, H.; Duering, R. Tianjin INSAR Time Series Analysis with L- and X-Band. In *Proceedings of the 2011 IEEE International Geoscience and Remote Sensing Symposium (IGARSS)*, Vancouver, BC, Canada, 24–29 July 2011; pp. 1477–1480.
5. Small, D.; Meier, E.; Jonsson, S.; Nuesch, D. ScanSAR InSAR processing of ASAR wide Swath SLC (WSS) products. *Proc. Inst. Electr. Eng. Radar Sonar Navig.* 2003, 150, 193–200.
6. Ferretti, A.; Savio, G.; Barzaghi, R.; Borghi, A.; Musazzi, S.; Novali, F.; Prati, C.; Rocca, F. Submillimeter accuracy of InSAR time series: Experimental validation. *IEEE Trans. Geosci. Remote Sens.* 2007, 45, 1142–1153. [CrossRef]
7. Ferretti, A.; Prati, C.; Rocca, F. Permanent scatterers in SAR interferometry. *IEEE Trans. Geosci. Remote Sens.* 2001, 39, 8–20. [CrossRef]
8. Özer, I.E.; van Leijen, F.J.; Jonkman, S.N.; Hanssen, R.F. Applicability of satellite radar imaging to monitor the conditions of levees. *J. Flood Risk Manag.* 2018, 12509, 1–16. [CrossRef]
9. Perissin, D.; Wang, T. Time-series InSAR applications over urban areas in China. *IEEE J. Sel. Top. Appl. Earth Obs. Remote Sens.* 2011, 4, 92–100. [CrossRef]
10. Costantini, M.; Falco, S.; Malvarosa, F.; Minati, F.; Trillo, F.; Vecchioli, F. Persistent scatterer pair interferometry: Approach and application to COSMO-SkyMed SAR data. *IEEE J. Sel. Top. Appl. Earth Obs. Remote Sens.* 2014, 7, 2869–2879. [CrossRef]
11. Wu, J.; Hu, F. Monitoring ground subsidence along the Shanghai Maglev zone using TerraSAR-X images. *IEEE Geosci. Remote Sens. Lett.* 2017, 14, 117–121. [CrossRef]
12. Chang, L.; Dollevoet, R.P.; Hanssen, R.F. Nationwide railway monitoring using satellite SAR interferometry. *IEEE J. Sel. Top. Appl. Earth Obs. Remote Sens.* 2017, 10, 596–604. [CrossRef]
13. Wang, H.; Chang, L.; Markine, V. Structural health monitoring of railway

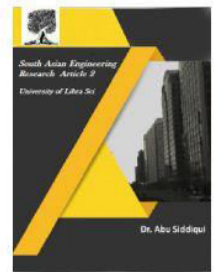


2581-4575

International Journal For Recent Developments in Science & Technology



A Peer Reviewed Research Journal



transition zones using satellite radar data. *Sensors* 2018, 18, 413. [CrossRef]

14. Ribeiro, D.; Calçada, R.; Ferreira, J.; Martins, T. Non-contact measurement of the dynamic displacement of railway bridges using an advanced video-based system. *Eng. Struct.* 2014, 75, 164–180. [CrossRef]